MODELING HYGROELASTIC PROPERTIES OF GENETICALLY MODIFIED ASPEN

Laszlo Horvath

Former PhD Student
E-mail: laszlo_horvath@vt.edu

Perry Peralta†

Associate Professor
E-mail: Perry_Peralta@ncsu.edu

Ilona Peszlen*†

Associate Professor
Department of Forest Biomaterials
North Carolina State University
Raleigh, NC 27695
E-mail: ilona_peszlen@ncsu.edu

Levente Csoka

Associate Professor
Faculty of Wood Sciences
University of West Hungary
Sopron, 9400 Hungary
E-mail: lcsoka@fmk.nyme.hu

Balazs Horvath

Former PhD Student
Department of Forest Biomaterials
North Carolina State University
Raleigh, NC 27695
E-mail: balihorvath@gmail.com

Joseph Jakes†

Research Materials Engineer
Performance Enhanced Biopolymers
USDA Forest Service, Forest Products Laboratory
1 Gifford Pinchot Drive
Madison, WI 53726
E-mail: jjakes@fs.fed.us

(Received June 2011)

Abstract. Numerical and three-dimensional finite element models were developed to improve understanding of major factors affecting hygroelastic wood properties. Effects of chemical composition, microfibril angle, crystallinity, structure of microfibrils, moisture content, and hydrophilicity of the cell wall were included in the model. Wood from wild-type and decreased-lignin transgenic aspen (*Populus tremuloides* Michx.) was used for experimental validation of the computer model. The model was able to predict longitudinal elastic modulus of microfibrils and woody cell walls. The difference in longitudinal elastic properties between wild-type and genetically modified aspen wood was predicted well

only when additional softening of hemicelluloses and amorphous cellulose of transgenic aspen was included in the model.

INTRODUCTION

Wood is a complex natural material that can be modeled at different organizational levels. At the macroscale, wood is an orthotropic heterogeneous material, whereas at the mesoscale, it can be considered a cellular solid composed of longitudinally oriented cells with diverse shapes (Gibson and Ashby 1999). Cells are connected by an isotropic matrix called the middle lamella. At the microscale, the cell wall can be divided into four layers with different properties: primary wall layer (P) and three layers of secondary wall (S1, S2, and S3). At the submicroscopic scale, the individual secondary cell wall layer is composed of parallel-oriented cellulose microfibrils (CMF) embedded in an amorphous matrix (Mark 1967). CMFs deviate from the cell longitudinal axis by an angle called microfibril angle (MFA). The CMF is composed of highly crystalline and less ordered amorphous parts, where amorphous cellulose is accessible to water and possesses characteristics similar to the matrix material (Salmen 2004; Hofstetter et al 2005). CMF is surrounded by polyoses such as the less branched xylan for hardwoods or glucomannan for softwood (Åkerholm and Salmén 2001). The amorphous matrix is composed of a hydrophobic and amorphous polymer called lignin and of hydrophilic and highly branched polymers called hemicelluloses (Hansen and Plackett 2008).

Numerous researches have dealt with prediction of softwood mechanical behavior in the micro- and mesoscale. The first models considered wood as a cellular material in which the cell wall was assumed homogeneous (Gillis 1972; Easterling et al 1982; Koponen et al 1991). The triple point of the hexagonal tracheid cell was used by Gillis (1972) to model elastic properties of earlywood. Later, Easterling et al (1982) and Koponen et al (1991) built a three-dimensional model using a hexagonal tracheid cell cross-section and incorporating the effect of rays on mechanical properties. Kahle and Woodhouse (1994) improved the model using microscopic photographs to incorporate irregular cell wall shape and organization. In general, the cellular model explained the effect of rays and different mechanical properties in the radial and tangential directions. However, the model failed to accurately predict elastic properties because the heterogeneous microstructure of the cell wall was not included.

Other models were developed to analyze effect of wood density and MFA on cell wall elastic properties (Cave 1969; Cave and Walker 1994; Hofstetter et al 2007; Sedighi-Gilani and Navi 2007). The microstructure of the cell wall was modeled using the laminate theory in which the secondary cell wall layers, primary wall, and middle lamella were modeled as individual entities. At different magnification scales, multistep homogenization models were applied by Hofstetter et al (2005, 2007) to obtain elastic properties of softwoods and hardwoods. The models included effect of cell wall constituents, amorphous and crystalline cellulose, MFA, density, and cell shape. However, they were not capable of modeling nonlinear behavior and fracture (Mishnaevsky and Qing 2008).

Complex multiscale models were also developed to link wood microstructure to macroscopic properties (Salmen and Deruvo 1985; Astley et al 1997, 1998; Harrington et al 1998; Bergander and Salmén 2002; Qing and Mishnaevsky 2009a). In addition to the effect of density, cell shape, and MFA, crystalline length and organization of cell wall constituents were considered in these models. They used the laminate theory of Chou et al (1972) combined with multistep homogenization or the Halpin-Tsai equations (Halpin and Kardos 1976) for

continuous (Bergander and Salmén 2002; Qing and Mishnaevsky 2009a) and discontinuous (Salmen and Deruvo 1985) fiber reinforcement to calculate elastic properties of cell wall layers. In contrast to other models, multiscale models were able to predict fracture, nonlinear, and time-dependent behaviors.

Mechanical behavior of wood is strongly dependent on environmental conditions such as temperature and moisture. Water uptake of wood depends on the number of available hydroxyl groups in the cell wall (Rowell and Banks 1985). Because of its structure, lignin has fewer hydroxyl groups than carbohydrates and thus imparts hydrophobic properties to wood. Cellulose is highly crystalline in nature, and most of its hydroxyl groups are used in intra- and interhydrogen bonding. Only amorphous cellulose and the surface of cellulose crystals are accessible to water (Rowell and Banks 1985). Because of their irregular, branched structure, hemicelluloses are highly accessible to water. Therefore, they have a major role in mechanical softening and dimensional stability of wood during moisture sorption.

One of the earliest multiscale models that included the effect of moisture was developed by Koponen et al (1989). In this model, the matrix material was responsible for hygromechanical properties. Yamamoto and Kojima (2002) and Kojima and Yamamoto (2004) investigated hygromechanical properties of wood. Based on a comparison of the analytical model and experimental results, they proposed the presence of a semicrystalline subdomain between crystalline and amorphous cellulose. The effect of matrix material and amorphous cellulose on hygromechanical properties of wood was also investigated by Salmen (2004) who reported that amorphous cellulose might have properties similar to hemicelluloses and has a major effect on transverse properties. In contrast to Yamamoto and Kojima (2002) and Salmen (2004), a coaxial cylinder model with ultrastructural homogenization (Neagu and Gamstedt 2007) and a finite element representative volume element (RVE) (Qing and Mishnaevsky 2009b) was built in

which cellulose was considered purely crystalline and thus not accessible to moisture.

There is a lack of knowledge on how proportions of wood polymers and interactions among them affect mechanical performance of wood and the cell wall (Salmén and Burgert 2008). To have a better understanding of the role of wood polymers on micromechanical properties of wood, modified (enzymatically, chemically, or genetically) wood materials need to be investigated (Salmén and Burgert 2008). Recent advances in genetic engineering allowed for selective modification of wood chemical components without altering cell morphology (Li et al 2003). Various anatomical, physical, and mechanical properties of genetically modified aspen have been investigated, and some very interesting differences have been found between transgenic materials and the control (Horvath 2009, 2010). These genetically modified tree clones offered a unique opportunity to investigate the hygroelastic behavior of wood. The overall objective of this study was to develop a computer model that incorporates chemical composition, crystallinity, MFA, and moisture content as input variables to predict hygroelastic properties of wood. Wood from wild-type and decreased-lignin transgenic aspen was used for experimental validation of the model.

MATERIALS AND METHODS

Computational Modeling

Structure and properties used for the computer model. Aspen has the most uniform structure among hardwoods, and therefore during the modeling process, fibers were assumed to be the only load-bearing elements of the wood. The compound middle lamella (CML) (primary wall plus middle lamella), S1, S2, and S3 were considered in the RVE of the cell assembly. The CML was composed of a randomly oriented network of short CMFs embedded in an isotropic lignin–hemicellulose matrix. Each secondary cell wall layer was considered a unidirectional fiber-reinforced lamina with parallel, continuous CMFs oriented at a certain MFA and embedded

Table 1.   Ultrastructural parameters and chemical composition of the cell wall of wild-type and transgenic aspen used for micromechanical and finite element computer models.

			Wild-type aspen				Transgenic aspen			
			CML	S1	S2	S3	CML	S1	S2	S3
	Cellulose (%)		7	35	48	45	7	35	57	45
Volume fraction[a]	Hemicelluloses (%)	Oriented	0	3	3.2	3.5	0	3	3.2	2.5
		Not oriented	21	27	28.8	31.5	21	27	28.8	32.5
	Lignin (%)		72	35	20	20	72	35	11	20
Microfibril angle (degrees)[a]			N.A.	60	18	75	N.A.	60	19.7	75
Cellulose crystallinity[b] (%)			83.5				72.4			
Thickness[c] (μm)			0.22	0.2	2.6	0.04	0.22	0.2	2.6	0.04
Fiber lumen diameter[d] (μm)			7.6				7.7			
Oven-dry specific gravity of the cell wall[b]			1.55				1.51			
	Cellulose[e] (%)		40				43			
Weight fraction of wood	Hemicelluloses[b] (%)		26				26			
	Lignin[e] (%)		20				15			
	Cellulose (%)		39				43			
Volume fraction of wood	Hemicelluloses (%)		27				27			
	Lignin (%)		23				17			

[a] Values of S2 cell wall layer by Horvath (2010) and compound middle lamella (CML), S1, and S3 cell wall layer by Qing and Mishnaevsky (2009a).
[b] Horvath (2010).
[c] Panshin et al (1970).
[d] Horvath (2009).
[e] Horvath et al (2010b).

in a lignin–hemicellulose matrix. The microfibrils were covered with a sheath of highly oriented hemicelluloses, which make up 10% of the volume fraction of all hemicelluloses. Non-oriented hemicelluloses (90% of total hemicelluloses) were mixed with lignin macromolecules to form the lignin–hemicellulose matrix.

A summary of ultrastructural properties used in this model is given in Table 1. Weight fractions of the chemical constituents of wood were obtained from analytical chemical measurements (Horvath et al 2010b) and from literature data (Li et al 2003). Values were converted to volume fractions of wood using Eq 1.

$$f_k = WF_k \frac{\rho_{CW}}{\rho_k} \qquad (1)$$

where WF_k is weight fraction of the kth chemical component, ρ_k is density of the kth chemical component (Hofstetter et al 2005), and ρ_{CW} is density of the cell wall at oven-dry condition (Horvath 2010). Volume fractions of chemical constituents of the S2 cell wall layer were obtained from volume fractions of wood chemical constituents at constant cell wall thicknesses, cell lumen diameter, cell shape, volume fraction of chemical constituents of S1 and S3 cell wall layers, and CML.

Elastic properties of chemical constituents. Input parameters for elastic properties of the main wood constituents are given in Table 2. Hemicelluloses and crystalline cellulose were considered transversely isotropic, whereas lignin and amorphous cellulose were considered isotropic (Katz et al 2008).

Effect of moisture on chemical constituents. In the model, only amorphous cellulose and hemicelluloses were accessible to moisture. Moisture dependence of elastic moduli was based on the work of Qing and Mishnaevsky (2009a).

Model building process. During the study, separate models were built for wild-type aspen and transgenic aspen with decreased lignin content taking into account their morphological, physical, and chemical features.

In the first step, numerical models were built to calculate elastic properties of microfibrils using three different schemes (Scheme 1, Scheme 2, and Scheme 3). Results of the schemes were

Table 2.   Elastic properties (E, G) and Poisson's ratio (ν) of major cell wall constituents at 12% MC used for the computer model.

Polymer	Engineering property	Value	Method[a]	Reference
Cellulose (transversely isotropic)	E_1 (GPa)	138	E	Mark (1967); Nishino et al (1995)
	E_2 (GPa)	27.2	M	Mark (1967)
	G_{12} (GPa)	4.4	M	Mark (1967)
	ν_{12}	0.235	P	Cave (1978)
	ν_{22}	0.48	P	Cave (1978)
Amorphous cellulose (isotropic)	E (GPa)	5		Eichhorn and Young (2001)
	G (GPa)	1.85		Eichhorn and Young (2001)
Hemicelluloses (transversely isotropic)	E_1 (GPa)	7.0	E	Cousins (1978)
	E_2 (GPa)	3.5	P	Bergander and Salmén (2002)
	G_{12} (GPa)	1.8	P	Bergander and Salmén (2002)
	ν_{12}	0.2	P	Åkerholm and Salmén (2001)
	ν_{22}	0.4	P	Salmen (2004)
Lignin (isotropic)	E (GPa)	2	E	Cousins (1978)
	ν	0.3	E	Bodig and Jayne (1982)

[a] E (experiment), M (molecular dynamics models), and P (based on phenomenological reasoning) (Qing and Mishnaevsky 2009a).

compared with experimental results from the literature. In the next step, properties of the microfibrils were used to model elastic properties of cell wall layers using the Halpin-Tsai equations (Halpin and Kardos 1976). The outcome of the model was compared with results of experiments conducted on our transgenic aspen and with data from the literature.

Effect of MFA, moisture content, crystallinity, microfibril structure, and chemical composition on elastic properties of the cell wall was investigated. In the third step, elastic properties of the cell wall layers were entered into a finite element RVE of the wood macrostructure to obtain the macromechanical properties of wood. The result of the finite element (FE) model was compared with the experimental result of macromechanical properties of the wild-type and transgenic aspen.

Elastic properties of cellulose microfibrils. Elastic properties of CMF were calculated using three schemes (Fig 1). In Schemes 1 and 2, CMF was represented as crystalline and amorphous cellulose oriented in series and in parallel, respectively. Elastic properties were calculated using rule of mixtures equations (Eqs 2-3) (Jones 1999):

$$P_{c,Voigt} = P_{crystalline}V_{crystalline} + \left(1 - V_{crystalline}\right)P_{amorphous} \quad (2)$$

$$R_{c,Reuss} = \frac{1}{\dfrac{V_{crystalline}}{R_{crystalline}} + \dfrac{1 - V_{crystalline}}{R_{amorphous}}} \quad (3)$$

where P represents the following properties: E_2, ν_{12}, and ν_{23}; and R represents the following properties: E_1 and G_{12}. In Scheme 3, CMFs were unidirectional discontinuous fibers embedded in an isotropic matrix. Elastic properties are described by the Halpin-Tsai equations (Eqs 4-5) (Halpin and Kardos 1976; Eichhorn and Young 2001):

$$H_c = \frac{H_{amorphous}\left(1 + \xi V_{crystalline}\theta\right)}{1 - V_{crystalline}\theta} \quad (4)$$

$$\theta = \frac{H_{crystalline} - H_{amorphous}}{H_{crystalline} + \xi H_{amorphous}} \quad (5)$$

where H represents elastic modulus E, shear modulus G, or Poisson's ratio ν. ξ is a continuity parameter that is related to the aspect ratio. ξ = 5 produced the best fit to experimental values and was recommended by Eichhorn and Young (2001).

Elastic properties of the lignin–hemicellulose matrix. The lignin–hemicellulose matrix was constructed with the assumption that hemicelluloses were isotropic discontinuous randomly oriented entities in an isotropic matrix of lignin. It was assumed that hemicelluloses had elastic
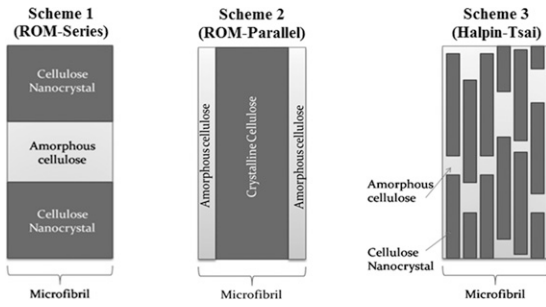
Figure 1. Representation of cellulose microfibril. Scheme 1: rule of mixtures in which crystalline and amorphous cellulose are in series along the length of the microfibril (ROM-series); Scheme 2: rule of mixtures in which crystalline and amorphous cellulose are parallel along the length (ROM-parallel); Scheme 3: Halpin-Tsai equations in which discontinuous short unidirectional nanocrystals are embedded in an isotropic matrix of amorphous cellulose (Halpin-Tsai).

modulus of 7 GPa and Poisson's ratio of 0.2 (Cousins 1978; Åkerholm and Salmén 2001). Elastic properties were calculated using the equations derived by Christensen and Waals (1972).

Elastic properties of secondary cell wall layers. In this model, a two-step homogenization using the Halpin-Tsai equations (Halpin and Kardos 1976; Horvath 2010) was used to obtain elastic properties of the secondary cell wall layers. In the first step, homogenization of cellulose and hemicelluloses resulted in homogeneous CMF properties. Then, the resulting homogeneous transversely isotropic fiber was embedded in an isotropic lignin–hemicellulose matrix to obtain homogenized secondary cell wall properties.

Elastic properties of compound middle lamella. Elastic properties of CML were calculated using two-step homogenization in which, first, effective properties of the lignin–hemicellulose matrix were calculated using the Christensen and Waals (1972) equations. Then, effective elastic properties of CML were obtained by embedding cellulose in the lignin–hemicellulose matrix using the Christensen and Waals (1972) equations

in which elastic modulus and Poisson's ratio of the cellulose were 134 GPa and 0.235, respectively.

Angle transformation. Elastic moduli for 0° MFA were obtained using the previously mentioned calculations. To calculate elastic moduli for MFA other than 0°, Eq 6 was used:

$$C'_{ij} = T_1^{-1}(\alpha) C_{ij} T_2(\alpha) \qquad (6)$$

where C_{ij} is stiffness matrix of the cell wall layer in the local or material coordinate system (1, 2, 3) where axis 1 is parallel whereas axes 2 and 3 are perpendicular to microfibril, C'_{ij} is transformed stiffness matrix in the global or geometric coordinate system (L, R, T) where axis L is parallel to axis of the fiber, α is MFA, and $T_1(\alpha)$, $T_2(\alpha)$ are transformation matrixes.

Macromechanical properties. A finite element RVE was designed to calculate macromechanical properties from elastic properties of each cell wall layer. The RVE represented the original structure of the wood by having S1, S2, and S3 secondary cell wall layers and CML. Linear tetrahedral element decreased integration points (C3D8R) of the Abaqus Finite Element Program were used for the model. Almost 200,000 elements were created using a structured meshing technique. Symmetric boundary condition was applied on the X-Y, Z-X, and Z-Y surfaces, whereas 0.5% displacement was applied on the top Z-Y surface.

Experimental Validation

Experimental measurements were conducted on young quaking aspen trees including one wild-type line as the control (PtrWT-271) and a transgenic group with decreased lignin content obtained through transfer of antisense 4CL gene (Ptr4CL). Sample trees were grown in the greenhouse of the Forest Biotechnology Group at North Carolina State University. A total of 50 sample trees were harvested between the ages of 1 and 2.5 yr. After harvest, sample trees were subjected to an extensive morphological, physical, and mechanical investigation (Horvath 2009; Horvath et al 2010b).

Table 3. Mean and coefficient of variation (COV) of mechanical and physical properties of wild-type and transgenic aspen with decreased lignin content.[a]

	Genetic group	Ptr WT (Wild-type)	Ptr 4CL (decreased lignin content)
	Genetic line	271	21 & 23 & 37
Modulus of elasticity at saturated condition	N	23	56
	Mean (MPa)	4902 A	2892 B
	COV (%)	12	12
Modulus of elasticity at oven-dry condition	N	17	55
	Mean (MPa)	8258 A	7246 B
	COV (%)	8	13
Modulus of elasticity DMA in water	N	7	10
	Mean (MPa)	2368 A	1063 B
	COV (%)	8	11
Modulus of elasticity DMA at oven-dry condition	N	7	10
	Mean (MPa)	3850 A	3220 B
	COV (%)	16	16
Modulus of elasticity nanoindentation ambient condition	N	18	34
	Mean (MPa)	11.4 A	8.1 B
	COV (%)	9.1	19.5

[a] N, number of specimens; The mean of genetic groups with common letters are not significantly different from each other as determined by Tukey multiple comparison test at $\alpha = 0.05$.
   DMA, dynamic mechanical analyzer.

Nanoindentation. To identify suitable areas for nanoindentation, cross-sections of each specimen were prepared for optical microscopy. Approximately 30-μm-thick sections were cut and examined without staining. Areas of reaction wood were identified and avoided. Sections were also used to assure that the cross-section was perpendicular to the fiber axis. Fiber walls were tested with a Hysitron (Minneapolis, MN) TriboIndenter equipped with a Berkovich probe. The nanoindentation procedure and analysis generally followed Jakes et al (2009). Specimens were prepared without embedment using a diamond knife fit in a rotary ultramicrotome (Jakes et al 2009). For these experiments, RH inside the nanoindentation enclosure was maintained between 39 and 47% using a glycerin–water bath. Temperature was not locally controlled inside the enclosure and ranged between 21 and 28°C during these experiments. Specimens were placed inside the enclosure a minimum of 48 h prior to experiments for conditioning. Indents were performed to maximum loads between 0.06 and 0.18 mN, depending on thickness of the fiber wall tested. The structural compliance method was used to remove edge effects and specimen-scale flexing following proce-

dures in Jakes et al (2008). All residual indents were imaged with a calibrated Quesant atomic force microscope (AFM) incorporated in the Triboindenter. ImageJ (Agoura Hills, CA) software was used to manually measure contact areas from these AFM images.

Three-point bending test. Specimens with a span–to-depth ratio of 15 were cut from harvested trees. A total of 154 specimens were measured at saturated condition and 132 at oven-dry condition using a modified microscale three-point bending test. Bending tests were conducted using an MTS Alliance RF/300 at a 1.27-mm/min crosshead speed. Deflection was measured based on crosshead movement. The experimental setup for the micromechanical bending test is described in greater detail in Kasal et al (2007) and Horvath et al (2010b). Results of the mechanical test are given in Table 3.

Dynamic mechanical analysis. The elastic modulus of approximately 1 mm thick × 20 mm long × 1-5 mm wide parallel-sided specimens was measured using a TA Instruments (New Castle, DE) Q800 dynamic mechanical analyzer (DMA) in static mode at a 2-N/min loading rate

with water as a plasticizer (Horvath et al 2010a). Results of the test are given in Table 3.

Elastic Properties of Microfibrils

Calculated elastic properties of microfibrils for wild-type aspen at oven-dry condition are given in Table 4. There was almost a 4-fold difference between longitudinal elastic modulus values of Scheme 1 and Scheme 2, which was caused by the difference in organization of amorphous and crystalline cellulose. Scheme 3 produced values between Schemes 1 and 2. Transverse modulus showed a trend opposite that of longitudinal elastic modulus. In-plane shear modulus (G_{12}) and Poisson's ratios for the three schemes were comparable.

In Fig 2, longitudinal elastic modulus of microfibrils is given as a function of crystallinity. The model predicts longitudinal elastic modulus increasing significantly with increasing crystallinity, which indicates that crystallinity had a significant effect on mechanical properties of microfibrils.

Schemes 1 and 2 represent the lower and upper bound for longitudinal modulus, respectively. Calculated values were compared with results of various experiments on microcrystalline cellulose, cellulose whisker, and bacterial cellulose. A longitudinal elastic modulus in three-point bending with AFM of 78 GPa was obtained by Guhados et al (2005) for bacterial cellulose with 60% crystallinity. Using the Raman tension test, Hsieh et al (2008) reported higher longitudinal elastic modulus (114 GPa)

for bacterial cellulose with 63-71% crystallinity. Lower (57 GPa) and upper (105 GPa) bounds were calculated by Rusli and Eichhorn (2008) for a single cellulose whisker with an aspect ratio of about 15 using Raman microtension and microcompression tests. A much lower modulus (25 GPa) using Raman bending tests was obtained for microcrystalline cellulose with crystallinity of about 45% (Eichhorn and Young 2001). Calculated values were in the same order of magnitude as the literature values. The lower bound for cellulose whiskers (57 GPa) and the modulus for microcrystalline cellulose (25 GPa) were close to those predicted by Scheme 3. Values for bacterial cellulose and the upper bound for cellulose whiskers were comparable with those predicted by Scheme 2.

Elastic Properties of the S2 Cell Wall Layer

Estimated elastic properties of the S2 cell wall layer of wild-type aspen at 12% MC and 0° MFA are given in Table 5. The highest longitudinal modulus was calculated by Scheme 2, whereas the lowest longitudinal modulus was calculated by Scheme 1. Longitudinal elastic modulus values of Schemes 1 and 3 were lower
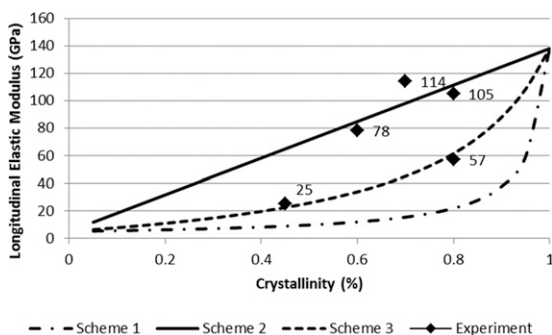

Figure 2. Predicted effect of cellulose crystallinity on properties of cellulose microfibrils of wild-type aspen at oven-dry condition. Scheme 1: rule of mixtures (series), Scheme 2: rule of mixtures (parallel), Scheme 3: Halpin-Tsai equations. 78 GPa: bacterial cellulose (Guhados et al 2005); 114 GPa: bacterial cellulose (Hsieh et al 2008); 105 and 57 GPa: cellulose whiskers (Rusli and Eichhorn 2008); 25 GPa: microcrystalline cellulose (Eichhorn and Young 2001).

Table 4. Calculated elastic properties (E, G) and Poisson's ratio (ν) of microfibrils of wild-type aspen at oven-dry condition at 84.3% crystallinity.[a]

	E_1 (GPa)	E_2 (GPa)	G_{12} (GPa)	ν_{12}	ν_{23}
Scheme 1	31.79	23.78	3.90	0.25	0.46
Scheme 2	116.30	17.82	3.89	0.25	0.46
Scheme 3	77.02	22.39	4.05	0.25	0.46

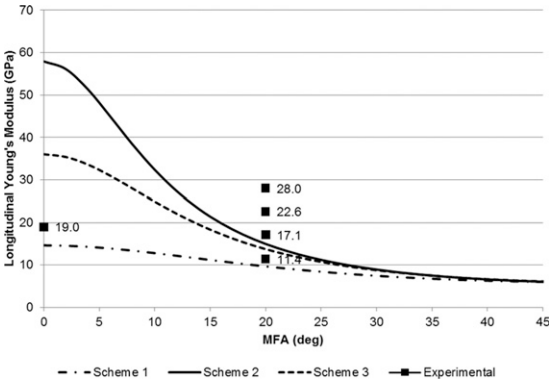[a] Scheme 1: rule of mixtures (series), Scheme 2: rule of mixtures (parallel), Scheme 3: Halpin-Tsai equations.

Table 5.   Calculated elastic properties (E, G) and Poisson's ratio (ν) of the S2 cell wall layer of wild-type aspen at 12% MC and 0° microfibril angle.[a]

	E_L (GPa)	E_R (GPa)	E_T (GPa)	G_{RT} (GPa)	G_{LT} (GPa)	G_{LR} (GPa)	ν_{RT}	ν_{LT}	ν_{LR}
Scheme 1	14.65	7.90	7.90	2.87	1.98	1.98	0.38	0.28	0.28
Scheme 2	57.93	6.83	6.83	2.48	1.98	1.98	0.38	0.28	0.28
Scheme 3	36.03	6.68	6.68	2.42	2.04	2.04	0.38	0.28	0.28

[a] Scheme 1: rule of mixtures (series), Scheme 2: rule of mixtures (parallel), Scheme 3: Halpin-Tsai equations.

Figure 3.   Predicted effect of microfibril angle (MFA) on calculated longitudinal modulus of the S2 cell wall layer of wild-type aspen. Scheme 1: rule of mixtures (series), Scheme 2: rule of mixtures (parallel), Scheme 3: Halpin-Tsai equations. 28 GPa: 19 GPa: nanoindentation (Gindl et al 2004); atomic force microscope microbending test (Orso et al 2006); 22.6 GPa: microtensile test (Burgert et al 2003, 2005); 11.4 GPa: nanoindentation (Table 3).

than previously reported values for numerical and finite element models, whereas that of Scheme 2 was comparable with these reported values (Harrington et al 1998; Bergander and Salmén 2002; Qing and Mishnaevsky 2009a; Qing and Mishnaevsky 2009b; Sedighi-Gilani and Navi 2007). The other elastic moduli and Poisson's ratios were not significantly affected by the use of different schemes.

The effect of MFA on longitudinal elastic modulus of the S2 layer of wild-type aspen at 12% MC is given in Fig 3. MFA had the greatest effect on longitudinal elastic modulus when Scheme 2 was used to calculate elastic properties of microfibrils. When Scheme 1 was used, MFA had only a minor effect on longitudinal modulus. MFA only had a significant effect between 0 and 45°. Above 45°, the effect of MFA was minor (data not shown).

Scheme 1 showed the best correlation with longitudinal elastic modulus of the S2 cell wall layer measured using nanoindentation for spruce with 0° MFA (19 GPa) (Gindl et al 2004) and for wild-type quaking aspen (11.40 GPa) (Table 3). However, when longitudinal modulus of spruce wood with 20° MFA (Gindl et al 2004) was investigated, Scheme 2 showed the best correlation. Meanwhile, other methods such as microbending by AFM (28 GPa) (Orso et al 2006) and microtensile test (22.6 GPa) (Burgert et al 2003, 2005) produced much higher longitudinal cell wall modulus. The higher modulus from microbending and microtension tests can be explained by the fact that during nanoindentation, the combination of longitudinal and transverse modulus is measured (Gindl et al 2004). Also, MFA of the cell wall used in the mentioned articles was only an approximation and was not backed up with experiments. Therefore, validation of the model requires experimental data with known MFA, crystallinity, moisture content, and chemical composition.

To show the effect of moisture, elastic moduli were normalized to 12% MC and are given in Fig 4. The result showed that moisture content has a similar effect on all elastic moduli investigated and did not depend significantly on the scheme used to calculate properties of the microfibril. Qing and Mishnaevsky (2009a) also investigated effect of moisture content on elastic properties and found that moisture content had a greater effect on transverse modulus than on longitudinal modulus. It is known that at low MFA, cellulose properties have a major effect on longitudinal elastic modulus, whereas transverse modulus is determined by properties of the matrix material. In the Qing and Mishnaevsky (2009a) model, cellulose was considered to be
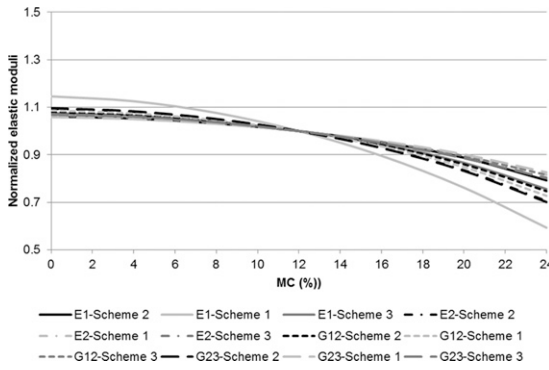
Figure 4.   Effect of moisture content on calculated elastic moduli of the S2 cell wall layer of wild-type aspen at 18° MFA. Scheme 1: rule of mixtures (series), Scheme 2: rule of mixtures (parallel), Scheme 3: Halpin-Tsai equations.

100% crystalline, whereas lignin was considered hydrophilic. However, in this model, the presence of hydrophilic amorphous cellulose in the microfibril increased hydrophilicity of the wood in the longitudinal direction.

Figure 5 presents the effect of chemical composition on longitudinal elastic modulus of aspen. The decrease in hemicellulose content and the corresponding increase in cellulose content caused an increase in longitudinal elastic modulus. This might have been caused by the reinforcing effect of cellulose.

The decrease in lignin and the corresponding increase in cellulose content showed an effect on longitudinal elastic modulus similar to the first case (decrease in hemicelluloses and increase in cellulose content). However, modification of lignin content had a greater effect on longitudinal elastic modulus than did hemicellulose. When lignin content decreased and hemicellulose content increased, the effect of moisture content on longitudinal elastic modulus was determined by changing chemical composition. With an increase in moisture content, the effect of lignin and hemicellulose content faded because of the fact that elastic moduli of lignin and hemicellulose were almost the same near the FSP. All these results indicated that if crosslinking effects were not considered and if every other factor was the same, longitudinal
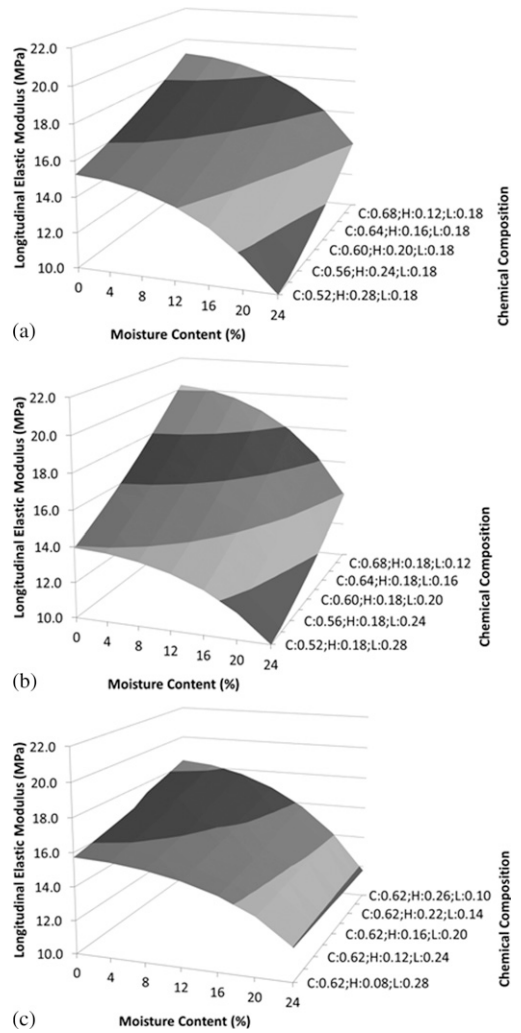

Figure 5.   Effect of modification of chemical constituents of the S2 cell wall layer of wild-type aspen on longitudinal elastic modulus as a function of moisture content. Decrease of hemicelluloses and corresponding increase in cellulose while lignin was constant (a), decrease of lignin and corresponding increase in cellulose while hemicelluloses were constant (b), decrease of lignin and corresponding increase in hemicelluloses while cellulose was constant (c). Amount of oriented hemicelluloses (10% of all hemicelluloses) was not changed. Scheme 3 (Halpin-Tsai equations) was used to calculate results at 20° microfibril angle.

elastic modulus should increase with decrease in lignin content. However, nanoindentation experiments and the micromechanical tests for wild-type and transgenic aspen at oven-dry and

saturated conditions (Table 3) showed that a decrease in lignin content and a corresponding increase in cellulose content decreased the longitudinal elastic modulus of the cell wall. At oven-dry condition, this might be attributed to the slight increase in MFA and decrease in crystallinity. However, the significant decrease in longitudinal elastic modulus at the saturated condition was not explained completely by these factors (Table 3). Therefore, it appeared that moisture had a greater effect on properties of the hydrophilic components of wood when lignin content decreased.

Based on Köhler and Spatz (2002) who worked on transgenic Arabidopsis with decreased lignin content, it was hypothesized that a decrease in lignin content will increase hydrophilicity of wood because of the greater number of accessible hydroxyl groups and therefore result in increased softening of hemicelluloses and amorphous cellulose. In addition, the reinforcing effect of lignin, which provides structural integrity to wood and controls moisture-related dimensional changes, might be decreased allowing deposition of multiple water layers between hemicelluloses and amorphous cellulose chains, thus resulting in increased softening of hemicelluloses and amorphous cellulose. Therefore, the combined effect of the increased number of accessible hydroxyl groups and the deposition of multiple water layers could be responsible for the significantly lower longitudinal elastic modulus of transgenic aspen at the saturated condition compared with the wild-type.

Possible effects of these factors on elastic moduli of hemicelluloses and amorphous cellulose are shown in Fig 6 in which five scenarios for moisture-induced softening are given. To calculate longitudinal elastic modulus of the S2 cell wall layer, Halpin-Tsai equations were used. Figure 7 presents results of additional softening by 10, 20, 30, and 40% on longitudinal elastic modulus. Schemes 1 and 2 provided an upper and lower boundary, whereas Scheme 3 resulted in a property between those of Schemes 1 and 2. A 40% additional softening resulted in a 60-72%
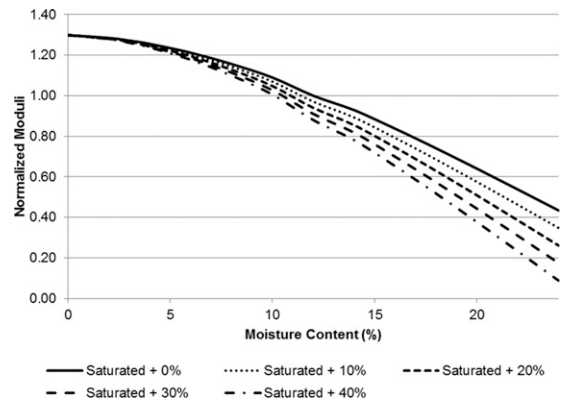

Figure 6. Dependence of amorphous cellulose and hemicelluloses on moisture content at various softening stages.
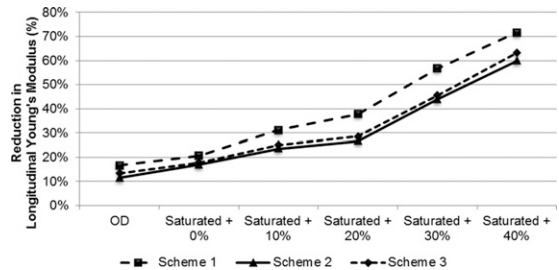

Figure 7. Effect of increased softening of hemicellulose and amorphous cellulose on calculated longitudinal elastic modulus for the S2 cell wall layer of wild-type and transgenic aspen at corresponding microfibril angle (wild-type: 18°; transgenic: 20°). Scheme 1: rule of mixtures (series); Scheme 2: rule of mixtures (parallel); Scheme 3: Halpin-Tsai equations.

difference in elastic properties of wild-type and transgenic aspen at FSP.

Macromechanical Properties

After elastic moduli of the individual cell wall layers of wild-type and transgenic aspen were calculated using Scheme 3, macromechanical elastic properties of the whole wood were calculated using a FE RVE at dry and saturated conditions. Calculated elastic moduli are given and compared with experimental values in Fig 8.

Calculated longitudinal elastic moduli (0% softening) of wild-type and transgenic aspen were lower than experimental longitudinal elastic
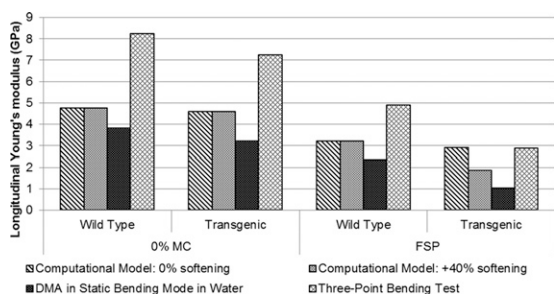
Figure 8. Trend of elastic properties of wild-type and transgenic aspen. Scheme 2 was used to calculate microfibril properties. Model 1-Halpin-Tsai was used for calculating cell wall properties.

modulus measured by three-point bending and were higher than longitudinal elastic modulus measured by DMA. The lower values produced by DMA measurements can be attributed to sample preparation (Horvath et al 2010a).

For wild-type aspen, increase in moisture content from 0% to FSP resulted in a 32% decrease in calculated longitudinal elastic modulus. This is in line with results of experiments using the three-point bending test (41%) and DMA with water as a solvent (38%). Published data (FPL 1999) show a 37% decrease in elastic modulus for mature quaking aspen when moisture increased from 12% to FSP.

Without additional softening, a 37% decrease in longitudinal elastic modulus was calculated for transgenic aspen when moisture content increased from 0% to FSP. This is lower than the decrease in experimental longitudinal elastic modulus (60% for three-point bending; 67% for DMA with water as a solvent). However, when 40% additional softening was incorporated in the model, the difference in predicted longitudinal elastic modulus of transgenic aspen between FSP and oven-dry condition (59%) was similar to that of experimental results. When longitudinal elastic modulus of wild-type aspen and that of transgenic aspen was compared at oven-dry condition, the FE model showed only a 3% difference, whereas differences of 14 and 20% were found in three-point bending tests and DMA experiments, respectively.

At FSP, the FE model using 0% softening underpredicted the difference between longitudinal elastic modulus of wild-type and transgenic aspen: 10% compared with experimental results of 69% difference for three-point bending and 124% difference for DMA in water. When softening was increased from 0-40%, the difference between longitudinal elastic modulus of wild-type and transgenic aspen (70%) was similar to experimental results.

SUMMARY AND CONCLUSION

Numerical and three-dimensional FE models were developed to calculate hygroelastic properties of genetically modified aspen wood. During model development, elastic properties were investigated at different organizational levels. Predicted elastic properties of microfibrils were in line with measured properties of bacterial cellulose when microfibrils were made of crystalline cellulose transversely connected to amorphous domains (Scheme 2). Good prediction of elastic properties of cellulose whiskers and microcrystalline cellulose was found when microfibrils were assembled by embedding finite-length crystalline cellulose in an amorphous cellulose domain (Scheme 3).

Predicted elastic modulus of the cell wall agreed with experimental results. Further improvement and validation of the model requires experimental data with known MFA, crystallinity, moisture content, and chemical composition. The computer model underestimated longitudinal elastic modulus of wood measured by three-point bending test. This indicated that mechanical properties of wood not only depended on the chemical, physical, and structural properties considered in this model, but also on the interaction among major wood polymers and other morphological features such as effect of rays, organization and shape of cells, and organization and shape of vessels.

The developed computer model predicted the difference between elastic properties of wild-type and transgenic aspen with decreased lignin content when additional softening of hemicelluloses

and amorphous cellulose of transgenic aspen were included to the effects of chemical composition, crystallinity, and MFA.

REFERENCES

Åkerholm M, Salmén L (2001) Interactions between wood polymers studied by dynamic FT-IR spectroscopy. Polymer (Guildf) 42(3):963-969.

Astley R, Harrington J, Stol K (1997) Mechanical modelling of wood microstructure, an engineering approach. Institution of Professional Engineers New Zealand Transactions 24(1):9.

Astley R, Stol K, Harrington J (1998) Modeling the elastic properties of softwood. Eur J Wood Wood Prod 56(1):43-50.

Bergander A, Salmén L (2002) Cell wall properties and their effects on the mechanical properties of fibers. J Mater Sci 37(1):151-156.

Bodig J, Jayne B (1982) Mechanics of wood and wood composites. Van Nostrand Reinhold, New York, NY. 736 pp.

Burgert I, Frühmann K, Keckes J, Fratzl P, Stanzl-Tschegg S (2003) Microtensile testing of wood fibers combined with video extensometry for efficient strain detection. Holzforschung 57(6):661-664.

Burgert I, Gierlinger N, Zimmermann T (2005) Properties of chemically and mechanically isolated fibres of spruce (*Picea abies* [L.] Karst.). Part 1: Structural and chemical characterisation. Holzforschung 59(2):240-246.

Cave I (1969) The longitudinal Young's modulus of *Pinus radiata*. Wood Sci Technol 3(1):40-48.

Cave I (1978) Modelling moisture-related mechanical properties of wood Part II: Computation of properties of a model of wood and comparison with experimental data. Wood Sci Technol 12(2):127-139.

Cave I, Walker J (1994) Stiffness of wood in fast-grown plantation softwoods: The influence of microfibril angle. Forest Prod J 44(5):43-48.

Chou P, Carleone J, Hsu C (1972) Elastic constants of layered media. J Composite Mater 6(1):80-93.

Christensen R, Waals F (1972) Effective stiffness of randomly oriented fibre composites. J Composite Mater 6(3):518-535.

Cousins W (1978) Young's modulus of hemicellulose as related to moisture content. Wood Sci Technol 12(3):161-167.

Easterling K, Harrysson R, Gibson L, Ashby M (1982) On the mechanics of balsa and other woods. Proc Royal Soc London. Series A, Mathematical and Physical Sci 383 (1784):31-41.

Eichhorn S, Young R (2001) The Young's modulus of a microcrystalline cellulose. Cellulose 8(3):197-207.

FPL (1999) Wood handbook: Wood as an engineering material. Gen Tech Rep FPL-GTR-113 USDA For Serv Forest Prod Lab, Madison, WI. 463 pp.

Gibson L, Ashby M (1999) Cellular solids: Structure and properties. Cambridge University Press, New York, NY. 510 pp.

Gillis P (1972) Orthotropic elastic constants of wood. Wood Sci Technol 6(2):138-156.

Gindl W, Gupta H, Schöberl T, Lichtenegger H, Fratzl P (2004) Mechanical properties of spruce wood cell walls by nanoindentation. Appl Phys A-Mater 79(8):2069-2073.

Guhados G, Wan W, Hutter J (2005) Measurement of the elastic modulus of single bacterial cellulose fibers using atomic force microscopy. Langmuir 21(14):6642-6646.

Halpin J, Kardos J (1976) The Halpin-Tsai equations: A review. Polym Eng Sci 16(5):344-352.

Hansen N, Plackett D (2008) Sustainable films and coatings from hemicelluloses: A review. Biomacromolecules 9(6):1493-1505.

Harrington J, Astley R, Booker R (1998) Modelling the elastic properties of softwood. Eur J Wood Wood Prod 56(1):37-41.

Hofstetter K, Hellmich C, Eberhardsteiner J (2005) Development and experimental validation of a continuum micromechanics model for the elasticity of wood. Eur J Mech A, Solids 24(6):1030-1053.

Hofstetter K, Hellmich C, Eberhardsteiner J (2007) Micromechanical modeling of solid-type and plate-type deformation patterns within softwood materials. A review and an improved approach. Holzforschung 61 (4):343-351.

Horvath B (2009) Effect of lignin content and structure on the anatomical, physical and mechanical properties of genetically engineered aspen trees. PhD dissertation, North Carolina State University, Raleigh, NC. 193 pp.

Horvath L (2010) Modeling the mechanical behavior of transgenic aspen with altered lignin content and composition. PhD dissertation, North Carolina State University, Raleigh, NC. 315 pp.

Horvath B, Peszlen I, Peralta P, Horvath L, Kasal B, Li L (2010a) Elastic modulus determination of transgenic aspen using a dynamic mechanical analyzer in static bending mode. Forest Prod J 60(3):296-300.

Horvath L, Peszlen I, Peralta P, Kasal B, Li L (2010b) Mechanical properties of genetically engineered young aspen with modified lignin content and/or structure. Wood Fiber Sci 42(3):310-317.

Hsieh Y, Yano H, Nogi M, Eichhorn S (2008) An estimation of the Young's modulus of bacterial cellulose filaments. Cellulose 15(4):507-513.

Jakes J, Frihart C, Beecher J, Moon R, Resto P, Melgarejo Z, Suárez O, Baumgart H, Elmustafa A, Stone D (2009) Nanoindentation near the edge. J Mater Res 24 (3):1016-1031.

Jakes J, Frihart C, Beecher J, Moon R, Stone D (2008) Experimental method to account for structural compliance in nanoindentation measurements. J Mater Res 23 (4):1113-1127.

Jones R (1999) Mechanics of composite materials. Taylor and Francis, Philadelphia, PA. 538 pp.

Kahle E, Woodhouse J (1994) The influence of cell geometry on the elasticity of softwood. J Mater Sci 29(5): 1250-1259.

Kasal B, Peszlen I, Peralta P, Li L (2007) Preliminary tests to evaluate the mechanical properties of young trees with small diameter. Holzforschung 61(4):390-393.

Katz J, Spencer P, Wang Y, Misra A, Marangos O, Friis L (2008) On the anisotropic elastic properties of woods. J Mater Sci 43(1):139-145.

Köhler L, Spatz H (2002) Micromechanics of plant tissues beyond the linear-elastic range. Planta 215(1): 33-40.

Kojima Y, Yamamoto H (2004) Properties of the cell wall constituents in relation to the longitudinal elasticity of wood. Wood Sci Technol 37(5):427-434.

Koponen S, Toratti T, Kanerva P (1989) Modelling longitudinal elastic and shrinkage properties of wood. Wood Sci Technol 23(1):55-63.

Koponen S, Toratti T, Kanerva P (1991) Modelling elastic and shrinkage properties of wood based on cell structure. Wood Sci Technol 25(1):25-32.

Li L, Zhou Y, Cheng X, Sun J, Marita J, Ralph J, Chiang V (2003) Combinatorial modification of multiple lignin traits in trees through multigene cotransformation. Proc Natl Acad Sci USA 100(8):4939-4944.

Mark R (1967) Cell wall mechanics of tracheids. Yale University Press, New Haven, CT. 310 pp.

Mishnaevsky L Jr, Qing H (2008) Micromechanical modelling of mechanical behaviour and strength of wood: State-of-the-art review. Comput Mater Sci 44(2):363-370.

Neagu R, Gamstedt E (2007) Modelling of effects of ultrastructural morphology on the hygroelastic properties of wood fibres. J Mater Sci 42(24):10254-10274.

Nishino T, Takano K, Nakamae K (1995) Elastic modulus of the crystalline regions of cellulose polymorphs. J Polym Sci Pol Phys 33(11):1647-1651.

Orso S, Wegst U, Arzt E (2006) The elastic modulus of spruce wood cell wall material measured by an in situ bending technique. J Mater Sci 41(16):5122-5126.

Panshin A, De Zeeuw C, Brown H (1970) Textbook of wood technology. McGraw-Hill, New York, NY. 736 pp.

Qing H, Mishnaevsky L (2009a) Moisture-related mechanical properties of softwood: 3D micromechanical modeling. Comput Mater Sci 46(2):310-320.

Qing H, Mishnaevsky L Jr (2009b) 3D hierarchical computational model of wood as a cellular material with fibril reinforced, heterogeneous multiple layers. Mech Mater 41(9):1034-1049.

Rowell R, Banks W (1985) Water repellency and dimensional stability of wood. Gen. Tech. Rep. FPL-GTR-50 USDA For Serv Forest Prod Lab, Madison, WI. 24 pp.

Rusli R, Eichhorn S (2008) Determination of the stiffness of cellulose nanowhiskers and the fiber-matrix interface in a nanocomposite using Raman spectroscopy. Appl Phys Lett 93(3):1-3 (Article Number 033111).

Salmen L (2004) Micromechanical understanding of the cell-wall structure. C R Biol 327(9-10):873-880.

Salmén L, Burgert I (2008) Cell wall features with regard to mechanical performance. A review COST Action E35 2004-2008: Wood machining: Micromechanics and fracture. Holzforschung 63(2):121-129.

Salmen L, Deruvo A (1985) A model for the prediction of fiber elasticity. Wood Fiber Sci 17(3):336-350.

Sedighi-Gilani M, Navi P (2007) Experimental observations and micromechanical modeling of successive-damaging phenomenon in wood cells' tensile behavior. Wood Sci Technol 41(1):69-85.

Yamamoto H, Kojima Y (2002) Properties of cell wall constituents in relation to longitudinal elasticity of wood. Wood Sci Technol 36(1):55-74.